Fission of hyper-hyperdeformed ^{56}Ni: a clustering analysis with in mean-field approaches

R.K. Gupta, S.K. Patra, C. Beck, W. Greiner

Fission of hyper-hyperdeformed ^{56}Ni: a clustering analysis with in mean-field approaches

Raj K. Gupta[a], S.K. Patra[b], P.D. Stevenson[c], C. Beck[d], and Walter Greiner[e]
[a] *Department of Physics, Panjab University, Chandigarh - 160 014 India*
[b] *Institute of Physics, Sachivalaya Marg, Bhubaneswar - 751 005, India*
[c] *Department of Physics, University of Surrey, Guildford, Surrey, GU2 7XH, UK*
[d] *Institut Pluridisciplinaire Hubert Curien, UMR7178, IN2P3/CNRS, Université Louis Pasteur, B.P. 28, F-67037 Strasbourg Cedex 2, France and*
[e] *Frankfurt Institute for Advanced Studies (FIAS), J.-W.-Goethe-Universität, Max-von-Laue-Str. 1, D-60438 Frankfurt am Main, Germany.*
(Dated: January 22, 2008)

The structure of ^{56}Ni is studied by using the non-relativistic Skyrme Hartree-Fock and the relativistic Hartree approximation in an axially deformed cylindrical coordinate. We found several intrinsic excited states, including the spherical ground-state solution. Without including any extra α-cluster correlations, the possible cluster configurations of the resonance states are analyzed, showing the multiple N=Z, α-nucleus like, cluster structures for hyper-deformed states, but, contrary to the recent experimental possibilty of a ternary fission decay, we predict a two cluster or symmetric fission configuration for the hyper-hyperdeformed state.

PACS numbers: 21.60.-n, 21.60.Gx, 24.10.Jv

I. INTRODUCTION

The compound nucleus ^{56}Ni* is a well studied system both experimentally and theoretically. In an early study, Betts [1, 2] measured the mass spectrum of the 75 and 80.6 MeV ^{16}O+^{40}Ca$\rightarrow^{56}$Ni*. A subsequent excitation function measurement of the ^{16}O+^{40}Ca reaction by Dichter *et al.* [3], confirming the previous results of [1, 2], indicates an explicit preference for α-nucleus (N=Z nuclei) transfer, which is best understood as a (binary) collective mass transfer in the dynamical fragmentation theory, using either the proximity pocket formula [4–6] or the nuclear potential based on the energy density formalism [7]. The same result of preferred α-nucleus fragments was observed in the ^{32}S+^{24}Mg entrance channel reaction at two incident energies, E_{lab}=121.1 and 141.8 MeV [8, 9], interpreted as the (statistical) emission of intermediate mass fragments (IMFs) from an equilibrated compound nucleus (CN) within the framework of the Extended Hauser-Feshbach Method (EHFM) [10], the scission point model, [EHFM is an extension of the Hauser-Feshbach formalism which gives a detailed analysis of the compound nucleus decay by emission of light particles n, p, α, and γ-rays], or (the emission of IMF's) as binary fission decay in a statistical saddle-point "transition-state" model (TSM) [8, 9, 11]. Alternatively, the IMF's are considered as the dynamical collective mass motion of preformed clusters through the barrier in a, so-called, dynamical cluster-decay model (DCM), also applied on equal footings to the emission of light particles n, p, and α [12]. Note that both the light particles and fission-like IMFs (or clusters) of α-nuclei constitute the CN fusion cross-section. The symmetric and asymmetric fission of ^{56}Ni has also been studied within the generalized liquid drop model, including the nuclear proximity energy and angular momentum effects [13]. Interestingly, quasi-molecular hyperdeformed configurations are obtained at sufficiently high angular momenta, which might correspond to some of the experimentally observed resonances [1, 2, 14, 15], while for lower spins the fission barriers are sufficiently high and wide to allow fusion-fission phenomena. In another study [16], the quasi-molecular resonance states in ^{28}Si+^{28}Si$\rightarrow^{56}$Ni* are shown to be of a di-nuclear configuration within a two-centre shell model description. Apparently, all these studies point to a binary fission or clustering process. In a very recent study, however, in addition to the pure binary events, ternary fission events with a missing (third) mass of 2 or 3α-particles are also observed [17] in an (unpublished) experiment of ^{32}S+^{24}Mg reaction at E_{lab}=163.5 MeV. Ternary fission was also found in the neighbouring ^{36}Ar+^{24}Mg reaction [18]. In the present paper, we look for the clustering structure of ^{56}Ni in both the ground and excited (resonance) states, using the two different mean-field approaches of non-relativistic Skyrme Hartree-Fock (SHF) and relativistic mean field (RMF). The question is: Do clusters exist in ^{56}Ni and, if yes, is its fissioning state just a binary-cluster state or of a ternary-cluster nature?

Alpha-particle and/ or α-nucleus clustering is a general feature of N=Z, $\alpha-$like nuclei in the light-mass region [19–21] and the RMF calculations are now known [22] to reproduce the $\alpha-$cluster as well as α- and non-α-nucleus cluster structures for light nuclei. In other words, the $\alpha-$nucleus structure is experimentally as well as theoretically well understood for N=Z, $\alpha-$nuclei. For example, in RMF approach, the ^{8}Be is shown to be of an α-α cluster structure [22]. Then, the ground state of ^{12}C is believed to correspond to a 3α-particles configuration in an equilateral triangle [23], distinctly supported by the above mentiond RMF calculation [22]. At a higher deformation β=2.33, the 3α linear chain structure for ^{12}C is also clearly seen in these RMF calculations [22]. In

^{16}O, the excited 0_2^+ state is predicted to be a coplanar configuration with $\alpha-$particles forming a kite-like structure [23, 24], once again seconded by the RMF formalism with a quadrupole deformation $\beta_2 = 0.95$ at an intrinsic excitation energy of 14.89 MeV [22]. Similarly, the α- and α-nucleus clustering structures of ^{20}Ne, ^{28}Si, ^{32}S and ^{36}Ar are well explained in several studies using either the α-cluster model [25–27] or the RMF formalism [22, 28], although the two approaches are very different conceptually. Then, there is also enough experimental evidence for the existence of extremely deformed oblate and triaxial cluster configurations in $A = 4n$ nuclei [27, 29, 30]. Thus, the above noted recent study of clustering structures in light nuclei using the RMF formalism [22], and the same in heavy, superheavy and super-superheavy nuclei [31–33] is rather a clear indication that the RMF is a suitable frame-work for studying the clustering structure of nuclei for all masses of the Periodic Table, and hence ^{56}Ni nucleus forms an interesting case from the heavier part of the light-mass region. Note that no explicit α-cluster correlations are addd here in the RMF analysis of α-nucleus structure in either the light, heavy, superheavy or super-superheavy nuclei.

The non-relativistic mean field formalism, like that of Skyrme Hartree-Fock (SHF), is also used for the clustering analysis of heavy, superheavy and super-superheavy nuclei [31, 33], but here the clustering effects are found to be not as apparent and universal as in RMF formalism. Once again, no α-cluster correlations were included in these calculations. Therefore, in view of the very good success of RMF method for light mass nuclei, it should be of interest to see the application of SHF method to light mass nuclei such as ^{56}Ni, and compare its results with the RMF results, for both the resonance and fissioning states. In other words, in this study, we aim at seeing the presence of α-cluster like correlations in SHF analysis of light mass nuclei, like the ones already found to exist in RMF method. Note that both the SHF and RMF theories are known to be equally successful for explaining the ground state properties.

II. THEORETICAL FRAMEWORK

A. The Skyrme Hartree-Fock (SHF) Method:

There are many known parametrizations of Skyrme interaction which reproduce the experimental data for ground-state properties of finite nuclei and for the observables of infinite nuclear matter at saturation densities, giving more or less comparable agreements with the experimental or expected empirical data. The general form of the Skyrme effective interaction, used in the mean-field models, can be expressed as a density functional $\mathcal{H}$ [34, 35], given as a function of some empirical parameters, as

$$\mathcal{H} = \mathcal{K} + \mathcal{H}_0 + \mathcal{H}_3 + \mathcal{H}_{eff} + \cdots + \ldots \qquad (1)$$

where $\mathcal{K}$ is the kinetic energy term, $\mathcal{H}_0$ the zero range, $\mathcal{H}_3$ the density dependent and $\mathcal{H}_{eff}$ the effective-mass dependent terms, which are relevant for calculating the properties of nuclear matter, are functions of 9 parameters t_i, x_i $(i = 0, 1, 2, 3)$ and η, given as

$$\mathcal{H}_0 = \frac{1}{4}t_0\left[(2+x_0)\rho^2 - (2x_0+1)(\rho_p^2+\rho_n^2)\right], \qquad (2)$$

$$\mathcal{H}_3 = \frac{1}{24}t_3\rho^\eta\left[(2+x_3)\rho^2 - (2x_3+1)(\rho_p^2+\rho_n^2)\right], \qquad (3)$$

$$\begin{aligned}\mathcal{H}_{eff} &= \frac{1}{8}\left[t_1(2+x_1)+t_2(2+x_2)\right]\tau\rho \\ &+\frac{1}{8}\left[t_2(2x_2+1)-t_1(2x_1+1)\right](\tau_p\rho_p+\tau_n\rho_n).\end{aligned} \qquad (4)$$

The kinetic-energy $\mathcal{K} = \frac{\hbar^2}{2m}\tau$, a form used in the Fermi gas model for non-interacting fermions. The other terms representing the surface contribution of a finite nucleus, with b_4 and b'_4 as additional parameters, are

$$\begin{aligned}\mathcal{H}_{S\rho} &= \frac{1}{16}\left[3t_1(1+\frac{1}{2}x_1) - t_2(1+\frac{1}{2}x_2)\right](\vec{\nabla}\rho)^2 \\ &-\frac{1}{16}\left[3t_1(x_1+\frac{1}{2}) + t_2(x_2+\frac{1}{2})\right] \\ &\times\left[(\vec{\nabla}\rho_n)^2 + (\vec{\nabla}\rho_p)^2\right].\end{aligned} \qquad (5)$$

$$\mathcal{H}_{S\vec{J}} = -\frac{1}{2}\left[b_4\rho\vec{\nabla}\cdot\vec{J} + b'_4(\rho_n\vec{\nabla}\cdot\vec{J_n} + \rho_p\vec{\nabla}\cdot\vec{J_p})\right]. \qquad (6)$$

Here, the total nucleon number density $\rho = \rho_n + \rho_p$ and kinetic energy density $\tau = \tau_n + \tau_p$, and the spin-orbit density $\vec{J} = \vec{J_n} + \vec{J_p}$. The subscripts n and p refer to neutron and proton, respectively, and m is the nucleon mass. The $\vec{J_q}$=0; q=n or p for spin-saturated nuclei, i.e., for nuclei with major oscillator shells completely filled. At least eighty-seven parametrizations of the Skyrme interaction are published since 1972 [36] where $b_4 = b'_4 = W_0$, but we have used here the Skyrme SkI4 set with $b_4 \neq b'_4$ [37]. This parameter set is designed for considerations of proper spin-orbit interaction in finite nuclei, related to the isotope shifts in Pb region. Several more recent Skyrme parameters such as SLy1-10, SkX, SkI5 and SkI6 are obtained by fitting the Hartree-Fock (HF) results with experimental data for nuclei starting from stability to neutron and proton drip-lines [34, 37–39]. However, for a stable nucleus like ^{56}Ni, SkI4 should be enough to illustrate our result. The pairing effects are added here within the standard BCS formalism, with the δ-force [40]. The total binding energy of a nucleus is the integral of the density functional $\mathcal{H}$.

B. The Relativistic Mean Field (RMF) Method:

The relativistic mean field approach is well-known and the theory is well documented [28, 41–47]. Here we start with the relativistic Lagrangian density for a nucleon-meson many-body system, as

$$\begin{aligned}\mathcal{L} &= \overline{\psi_i}\{i\gamma^\mu\partial_\mu - M\}\psi_i + \frac{1}{2}\partial^\mu\sigma\partial_\mu\sigma - \frac{1}{2}m_\sigma^2\sigma^2 \\ &-\frac{1}{3}g_2\sigma^3 - \frac{1}{4}g_3\sigma^4 - g_s\overline{\psi_i}\psi_i\sigma - \frac{1}{4}\Omega^{\mu\nu}\Omega_{\mu\nu} \\ &+\frac{1}{2}m_w^2V^\mu V_\mu + \frac{1}{4}c_3(V_\mu V^\mu)^2 - g_w\overline{\psi}_i\gamma^\mu\psi_iV_\mu \\ &-\frac{1}{4}\vec{B}^{\mu\nu}.\vec{B}_{\mu\nu} + \frac{1}{2}m_\rho^2\vec{R}^\mu.\vec{R}_\mu - g_\rho\overline{\psi}_i\gamma^\mu\vec{\tau}\psi_i.\vec{R}^\mu \\ &-\frac{1}{4}F^{\mu\nu}F_{\mu\nu} - e\overline{\psi}_i\gamma^\mu\frac{(1-\tau_{3i})}{2}\psi_iA_\mu. \qquad (7)\end{aligned}$$

All the quantities have their usual well known meanings. From the relativistic Lagrangian we obtain the field equations for the nucleons and mesons. These equations are solved by expanding the upper and lower components of the Dirac spinors and the boson fields in an axially deformed harmonic oscillator basis with an initial deformation. The set of coupled equations is solved numerically by a self-consistent iteration method. The baryon (vector), scalar, isovector and proton densities are, respectively, as

$$\rho(r) = \sum_\alpha \varphi_\alpha^\dagger(r)\varphi_\alpha(r)\,, \qquad (8)$$

$$\rho_s(r) = \sum_\alpha \varphi_\alpha^\dagger(r)\beta\varphi_\alpha(r)\,, \qquad (9)$$

$$\rho_3(r) = \sum_\alpha \varphi_\alpha^\dagger(r)\tau_3\varphi_\alpha(r)\,, \qquad (10)$$

$$\rho_{\rm p}(r) = \sum_\alpha \varphi_\alpha^\dagger(r)\left(\frac{1+\tau_3}{2}\right)\varphi_\alpha(r)\,. \qquad (11)$$

The centre-of-mass motion energy correction is estimated by the usual harmonic oscillator formula $E_{c.m.} = \frac{3}{4}(41A^{-1/3})$. The quadrupole deformation parameter β_2 is evaluated from the resulting proton and neutron quadrupole moments, as $Q = Q_n + Q_p = \sqrt{16\pi/5}(3/4\pi AR^2\beta_2)$ [42, 43]. The root mean square (rms) matter radius is defined as $< r_m^2 >= \frac{1}{A}\int\rho(r_\perp,z)r^2d\tau$; here A=mass number, and $\rho(r_\perp,z)$ is the deformed density [43]. The total binding energy and other observables are also obtained by using the standard relations, given in [42]. We use here the well known NL3 parameter set [48]. The NL3 set not only reproduces the properties of stable nuclei but also well predict for those far from the $\beta-$stability valley. Also, the isoscalar monopole energy agrees excellently with the experimental values for different regions of the Periodic Table. The measured superdeformed minimum in ^{194}Hg is 6.02 MeV above the ground [49] whereas in RMF calculation with NL3 set this number is 5.99 MeV [48]. All these facts give us confidence to use this older, though very much still in use, NL3 set for the present investigation.

As outputs, we obtain different potentials, densities, single-particle energy levels, radii, deformations and the binding energies. For a given nucleus, the maximum binding energy corresponds to the ground state and other solutions are obtained as various excited intrinsic states. For studying the clustering aspects and subsequently the decay mode of various resonance states, the densities and quadrupole deformations are very important. The proton, neutron and matter densities are obtained in the positive quadrant of the plane parallel to the symmetry axis. As we choose z-axis as the symmetry axis, the densities are evaluated in the $z\rho$ plane, where $x = y = \rho$. As the space reflection symmetry about z-axis, as well as ρ axes, is conserved in our formalism, the results obtained in the positive quadrant are suitably reflected in other quadrants so as to have a complete picture in the $z\rho$ plane. Such unbroken symmetries of our numerical procedure leads to several limitations, which are discussed in our earlier work [22].

III. CALCULATIONS AND RESULTS

First of all, we have calculated the potential energy surface (PES) for ^{56}Ni, using the Skyrme Hartree-Fock (SHF) method with SkI4 parameter set [36]. Since all the local minima, including the ground state configuration, exist in a multi-deformed space, we take into account the effects of quadrupole, octopole and hexadecapole deformations in both the SHF and RMF calculations. The calculated PES for SHF is shown in Fig. 1 for a wide range of oblate to prolate deformations. We notice from this figure that minima appear at $\beta_2 \sim -0.6$, 0.0, 0.4 and 1.8. Considering these minima as the precurcers for the ground and intrinsic excited isomaric states, we looked for different solutions in different regions of the PES, using both the RMF and SHF formalisms. The different solutions found at various quadrupole deformations β_2 with different intrinsic binding energies B.E., as well as the matter radii r_m are listed in Table I. The pairing correlations could be ignored here, since ^{56}Ni, with N=Z=28, is a double magic nucleus. However, we found the role of pairing when we performed our SHF and RMF calculations with and without pairing taken into account (see Table I). Interestingly, in the RMF model calculations, the intrinsic minima, except the spherical ground state, are washed-out with the BCS constant-gap pairing switched-on. The small barriers (or shallow minima) at β_2 =-0.598, 0.403 and 1.828 become smooth by adding pairing interactions in the RMF calculations. In the SHF calculations, however, only the oblate solution disappears with pairing included. This means that the results of RMF calculations are very sensitive to pairing and are almost insensitive for the SHF model. On the other hand,

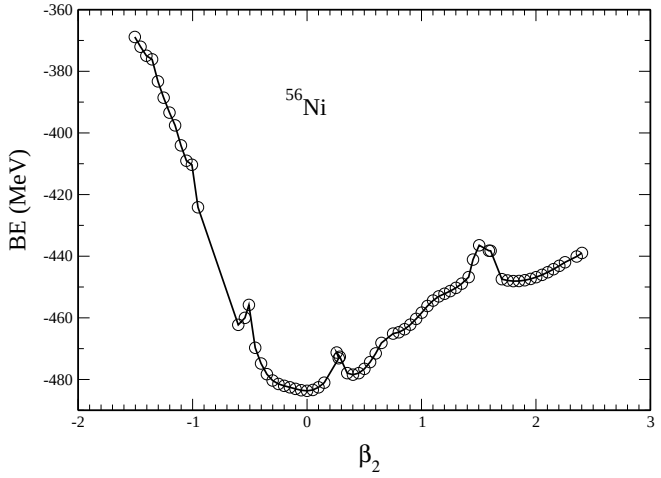

FIG. 1: The potential energy surface for ^{56}Ni using SkI4 force in SHF method.

TABLE I: Calculated binding energies (B.E.), deformation parameters (β_2) and matter distribution radii (r_m) for ^{56}Ni, using RMF (NL3 parameter set) and SHF (SkI4 set). The binding energy is in MeV and the radius r_m is in fm.

	B.E.(MeV)	β_2	r_m
SHF			
without pairing	462.292	-0.598	3.967
	483.826	0.000	3.639
	478.683	0.403	3.769
	448.968	1.828	4.697
	437.184	2.846	5.423
	400.776	5.748	7.225
with pairing	483.711	0.001	3.639
	478.812	0.404	3.768
	437.304	2.810	5.401
	415.124	4.874	6.730
	412.056	8.882	8.777
RMF			
without pairing	461.218	-0.583	3.918
	482.562	0.000	3.601
	475.803	0.405	3.760
	435.749	2.453	5.145
with pairing	482.865	-0.000	3.698

comparing the SHF and RMF results of Table 1 in the absence of pairing, we notice that both the models predict similar solutions (equivalent quadrupole deformation parameters at almost the same excitation energies). Also, knowing that pairing makes an important contribution only for open shell nuclei, and it could be ignored for a doubly closed shell nucleus like ^{56}Ni, we should analyze our results for the case of pairing not taken in to account. In other words, in order to get a comparable analysis of the two formalisms for clustering effects, in the following we proceed further without taking the pairing effects into account.

In Fig. 2, the density distribution for the total (proton+neutron) matter is depicted for the various outputs obtained in SHF calculations. Looking at the colour

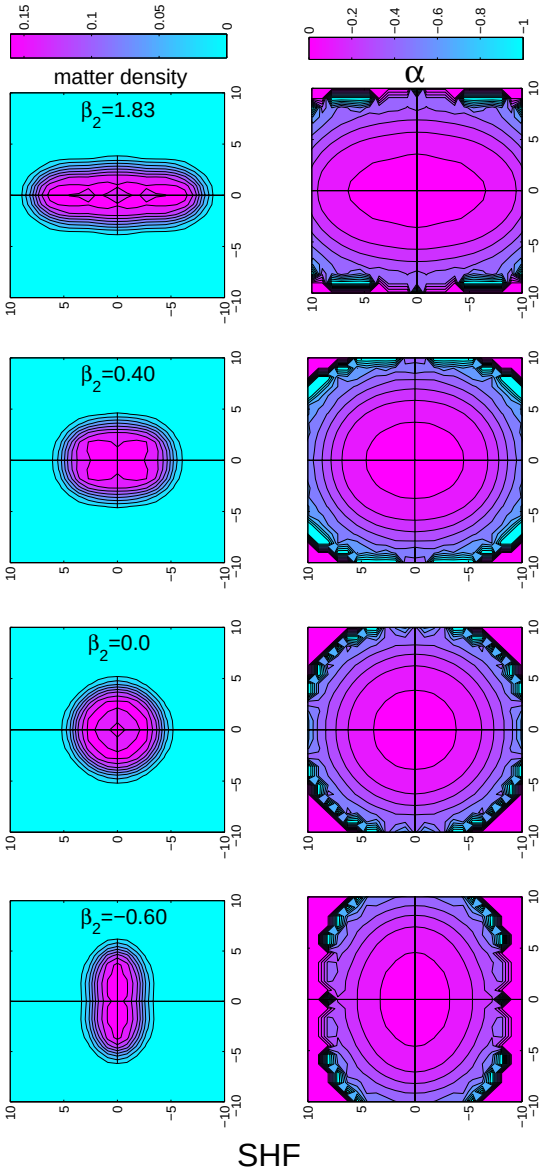

FIG. 2: (Color on line) The total (neutron+proton) density distribution for various solutions of ^{56}Ni using SkI4 force parameters in SHF formalism. The asymmetry parameter $\alpha = (\rho_n - \rho_p)/(\rho_n + \rho_p)$ is also shown. The contours are drawn in a square box of size 20 fm.

code, it is evident from this figure that the central part has the largest density distribution (∼0.1, with red in colour), with a maximum of three distinct clusters for the hyper-deformed, β_2=1.828 solution, which looks very similar to the ^{16}O-^{16}O-^{16}O configuration predicted by the Bloch-Brink α-cluster model for the hyper-deformed state of ^{56}Ni [26]. Interestingly, the superdeformed oblate solution is divided into two major clusters with a neck in the middle, and the spherical ground-state solution has a low density distribution of nucleons at the centre followed by a highly dense coating. Similar to superdeformed

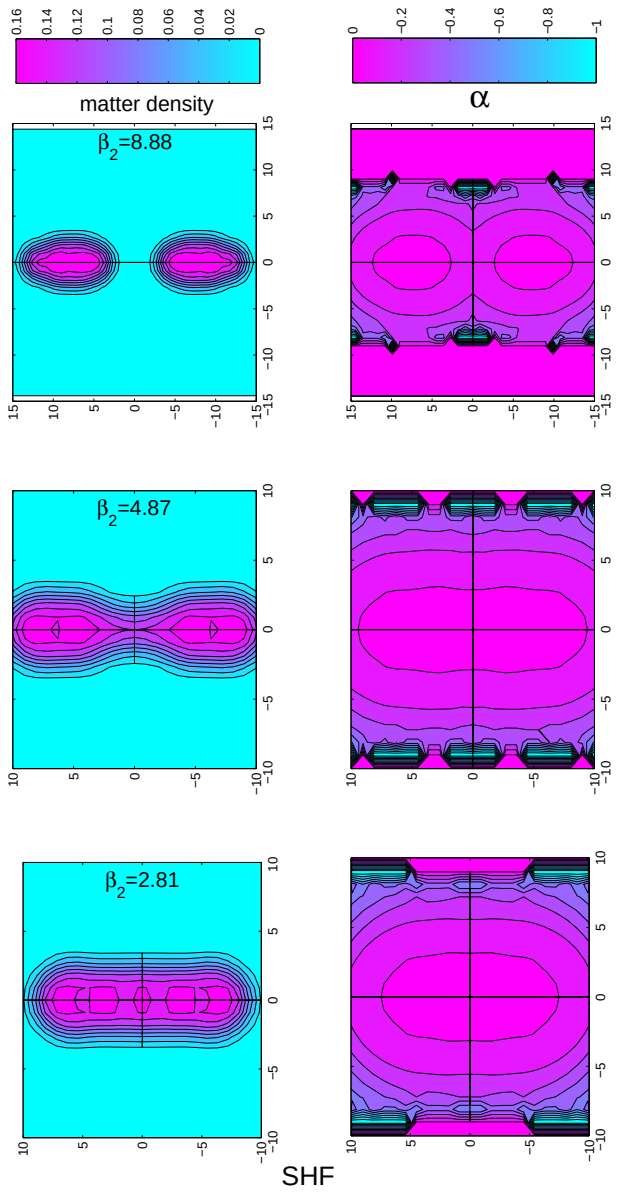

FIG. 3: (Color on line) The same as for Fig.2, but for higher deformations, including the hyper-hyperdeformed fissioning stage. The contours are drawn in a square box of size 20 fm.

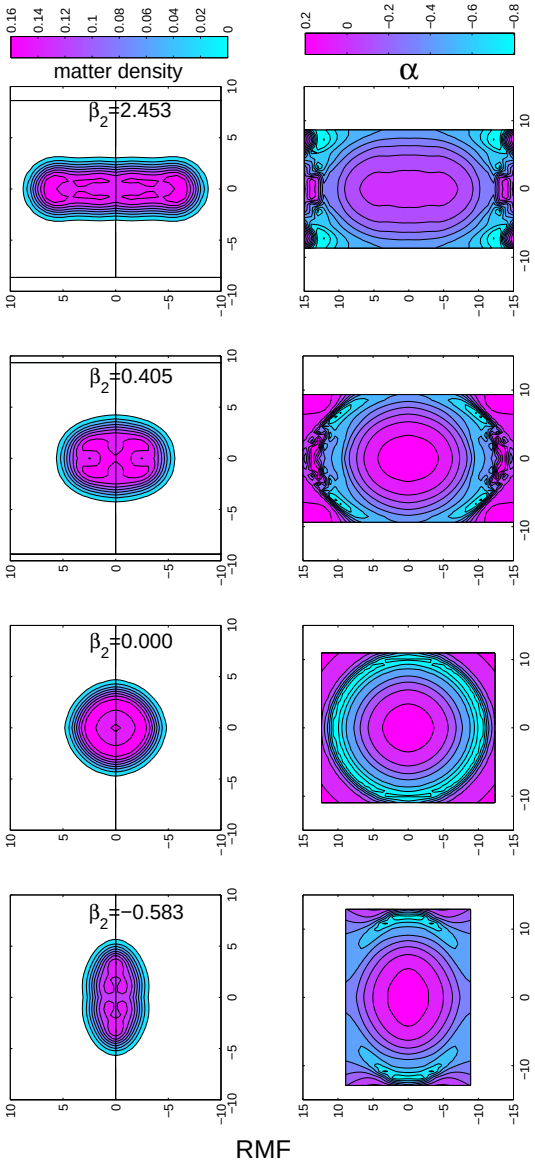

FIG. 4: (Color on line) The total (neutron+proton) density distribution and the asymmetry parameter α for various solutions of ^{56}Ni using NL3 force parameters in RMF calculations. The contours are drawn in a square box of size 20 fm.

oblate solution, the prolate deformed solution (β_2=0.40) also has a dense two cluster configuration at the middle, surrounded by a lesser dense medium. Note that the superdeformed oblate solution (so also for RMF in Fig. 4) would correspond to the well known resonance observed for the ^{28}Si+^{28}Si reaction [14, 15], in agreement with the prediction of an oblate-oblate superdeformed configuration in molecular model of Uegaki and Abe [50].

In order to see the neutron-proton ratio of the density distribution, we defined an asymmetry parameter $\alpha = (\rho_n - \rho_p)/(\rho_n + \rho_p)$ which is depicted on the right side of Fig. 2. Here, ρ_n and ρ_p are the neutron and proton density distributions, respectively. Apparently, $|\alpha|$=1 means only one type of nucleons (protons or neutrons), and $|\alpha|$=0 represents the N=Z, (α-nucleus type) symmetric nuclear matter. The intermediate values of α between 0 and 1 give the asymmetric matter. From the analysis of the asymmetry parameter α on the r.h.s. of Fig. 2, we find that one type of nucleons on the surface (mostly protons, since α ∼-1 in the surface region) surround the N=Z symmetric nuclear matter in the bulk central region. The nucleons seem to be distributed as a layer after layer on top of each other. In other words, in all the 4 solutions, the central part contains a pure N=Z

symmetric nuclear matter, followed by a slightly asymmetric nucleon layer which goes on increasing such that at the surface only a thick layer of pure nucleons (protons or neutrons) appears. Thus, the one, two or three cluster structures, respectively, of spherical, deformed or superdeformed (prolate/ oblate) or hyper-deformed shapes are all of pure N=Z, α-nucleus type matter.

Fig. 3 shows the matter density and asymmetry parameter calculations for higher deformations, leading towards a hyper-hyperdeformed fission configuration. Interestingly, at β_2=2.81, the matter spreads into a multiple α-nucleus cluster system, a result in complete agreement with the early experiments [1, 2], old calculations based on dynamical fragmentation theory [4–6], and even the new experiments [8, 9] and their theoretical understanding in terms of the dynamical cluster-decay model [12], mentioned above in the Introduction. As the deformation increases, at β_2=4.87 the multi-cluster structure culminates back into two big clusters, separated by a narrow neck. The two clusters then go on separating from each other and get completely separated in to two major binary products at β_2 = 8.88 with no emission of a smaller product. If one examines the asymmetry parameter contour plots for the subsequent deformations, the N=Z matter appears at the centre for β_2 =2.81 and β_2=4.87. This N=Z symmetric nuclear matter is surrounded by more asymmetric layers which get elongated gradually with the increase of deformation, and finally separated into two fragments without predicting any ternary fission, contradicting the (unpublished) experimental observation [17]. In addition to the main binary products, however, a highly neutron/proton-rich matter clearly exists in the fission state.

In Fig. 4, l.h.s., we have shown the matter density contour plots for the RMF solutions obtained with NL3 parameter set at various excitation energies. Similar to the case of SHF, the RMF calculations also give the four solutions of smaller deformations with highly dense clusters visible in the central region. In the superdeformed oblate case, two highly dense clusters appear, whereas for the spherical ground state solution, like for SHF, the centre is a thin layer of nucleons sourrounded by a higher density thick layer. The density distribution for β_2=0.405 also show two distinct clusters surrounded by a thin layer of nucleons. The cluster formation gets more and more pronounded with the increase of deformation, giving six distinctly visible clusters for β_2=2.453. The density distribution in this case is very elongated, with a clear multi-fragmentation or multiple-clusterization, like in SHF for β_2=2.81. The asymmetry parameter α plots on the r.h.s. of Fig. 4 clearly show an N=Z matter at the centre, surrounded by a slight asymmetric matter, for the three β_2=-0.583, 0.0 and 0.405 solutions. On the other hand, for the hyper-deformed β_2=2.453 case, the central part deviates slightly from the symmetric nuclear matter property, i.e., the middle portion has an asymmetric nuclear matter, surrounded by several layers of nucleons. The surface in each of the solutions is enriched by one type of nucleon matter. The RMF calculations, however, did not give the fission-like configuration at a still higher deformation, like the same could not be obtained in SHF calculation for super-superheavy compound nucleus ^{476}184 [33]. Apparently, both the SHF and RMF calculations support the multiple α-nucleus (not necessarily α-particle) cluster structure of ^{56}Ni, like the preferential α-nucleus decay observed in many experiments [1–3, 8, 9, 14, 15], and leads to symmetric fission or two cluster configuration, instead of ternary fission, in the final state of hyper-hyperdeformation.

IV. SUMMARY

In summary, we have studied the clustering phenomena in ^{56}Ni nucleus at various intrinsic isomeric states, where some of them are the molecular resonance states. The clustering phenomena is clearly visible in both the RMF and SHF formalisms, although the two approaches are very different from the alpha-cluster model [25–27] or other methods such as Fermionic molecular dynamics (FMD) [51] and antisymmetrized molecular dynamics (AMD) [20] whose results are very encouraging for N=Z exotic nuclei. While analyzing the matter density distributions of various intrinsic states, we found multiple α-nucleus like cluster structures in ^{56}Ni, without adding any explicit α-cluster correlations from outside. Both the models, however, failed to give the ternary fission at the hyper-hyperdeformed fissioning configuration, contrary to the recent experimental possibilities. However, the multiple α-nucleus clusterization is in agreement with many earlier experiments. There is still some scope in the present models to take into account the parity reflection symmetry and correlations beyond the mean field, which may be a greater limitation at present.

[1] R.R. Betts, *Proc. Conf. on Resonances in Heavy Ion Reactions*, Bad-Hönnef (Lecture Notes in Physics, Vol. 156), ed. K.A. Eberhardt, Berlin, Springer 1981, p. 185.

[2] R.R. Betts, *Proc. 5th Adriatic Int. Conf. on Nucl. Phys.*, Hvar (Fundamental Problems in Heavy Ion Collisions), ed. N. Cindro, *et al.*, Singapore, World Scientific 1984, p. 33.

[3] B.K. Dichter, P.D. Parker, S.J. Sanders, R.R. Betts, and S.Saini, Phys. Rev. C **35**, 1304 (1987).

[4] R.K. Gupta, N. Malhotra, and D.R. Saroha, *Proc. 4th Int. Conf. on Nuclear Reaction Mechanism*, Varenna, Ed. E. Gadioli, Milan, Universitá di Milano Press, June 1985.

[5] D.R. Saroha, N. Malhotra, and R.K. Gupta, J. Phys. G: Nucl. Phys. **11**, L27 (1985).

[6] S.S. Malik and R.K. Gupta, J. Phys. G: Nucl. Phys. **12**, L161 (1986).

[7] R.K. Puri and R.K. Gupta, J. Phys. G: Nucl. Part. Phys. **18**, 903 (1992).

[8] S.J. Sanders, D.G. Kovar, B.B. Back, C. Beck, D.J. Henderson, R.V.F. Janssens, T.F. Wang, and B.D. Wilkins, Phys. Rev. C **40**, 2091 (1989).

[9] S.J. Sanders, D.G. Kovar, B.B. Back, C. Beck, B.K. Dichter, D. Henderson, R.V.F. Janssens, J.G. Keller, S. Kaufman, T.-F. Wang, B. Wilkins, and F. Videbaek, Phys. Rev. Lett. **59**, 2856 (1987).

[10] T. Matsuse, C. Beck, R. Nouicer, and D. Mahboub, Phys. Rev. C **55**, 1380 (1997).

[11] S.J. Sanders, A. Szanto de Toledo, and C. Beck, Phys. Rep. **311**, 487 (1999).

[12] R.K. Gupta, M. Balasubramaniam, R. Kumar, D. Singh, C. Beck, and W. Greiner, Phys. Rev. C **71**, 014601 (2005); and earlier references there in it.

[13] G. Royer, J. Phys. G: Nucl. Part. Phys. **21**, 249 (1995).

[14] R. Nouicer, C. Beck, R.M. Freeman, F. Haas, N. Aissaoui, T. Bellot, G.de France, D. Disdier, G. Duchene, A. Elanique, A. Hachem, F. Hoellinger, D. Mahboub, V. Rauch, S.J. Sanders, A. Dummer, F.W. Prosser, A. Szanto de Toledo, Sl. Cavallaro, E. Uegaki, and Y.Abe, Phys.Rev. C **60**, 041303 (1999).

[15] C. Beck, R. Nouicer, D. Disdier, G. Duchne, G. de France, R. M. Freeman, F. Haas, A. Hachem, D. Mahboub, V. Rauch, M. Rousseau, S. J. Sanders, and A. Szanto de Toledo, Phys. Rev. C **63**, 014607 (2000).

[16] H.S. Khosla, S.S. Malik and R.K. Gupta, Nucl. Phys. **A513**, 115 (1990).

[17] G. Efimov, V. Zherebchevsky, W. von Oertzen, B. Gebauer, S. Thummerer, Tz. Kokalova, Ch. Schulz, H.G. Bohlen, D. Kamanin, C. Beck, D. Curien, M. Rousseau, P. Papka, G. Royer, G. de Angelis (2007) Preprint IPHC-07-007; http://hal.in2p3.fr/in2p3-00169805/fr/

[18] V. Zherebchevsky, W. von Oertzen, D. Kamanin, B. Gebauer, S. Thummerer, Ch. Schulz, and G.Royer, Phys. Lett. B **646**, 12 (2007).

[19] K. Ikeda, N. Takigawa and H. Horiuchi, Prog. Theo. Phys. Suppl. Extra No. 464 (1968);

[20] Y.K. Kanada-En'yo and H. Horiuchi, Phys. Rev. C **68**, 014319 (2002).

[21] C. Beck, Nucl. Phys. A **738**, 24 (2004); Int. J. Mod. Phys. E **13**, 9 (2004); and earlier references therein.

[22] P. Arumugam, B.K. Sharma, S.K. Sharma and R.K. Gupta, Phys. Rev. C **71**, 064308 (2005).

[23] P. Descouvemont, Phys. Phys. C **44**, 306 (1991).

[24] W. Bouhoff, H. Schultheis and R. Schulthesis, Phys. Phys. C **29**, 1046 (1984).

[25] J. Zhang and W.D.M. Rae, Nucl. Phys. A **564**, 252 (1993).

[26] J. Zhang, W.D.M. Rae and A.C. Merchant, Nucl. Phys. A **575**, 61 (1994); J. Zhang, A. C. Merchant, and W. D. M. Rae, Phys. Rev. C **49**, 562 (1994).

[27] W.D.M. Rae, Int. J. Mod. Phys. A **3**, 1343 (1988).

[28] M. Bender, P.-H. Heenen, and P.-G.Reinhard, Rev. Mod. Phys. **75**, 121 (2003).

[29] M. Freer and A. C. Merchant, J. Phys. G **23**, 261 (1997).

[30] R R Betts and A H Wuosmaa, Rep. Prog. Phys. **60**, 819 (1997).

[31] S.K. Patra, R.K. Gupta, B.K. Sharma, P.D. Stevenson and W. Greiner, J. Phys. G: Nucl. Part. Phys. **34**, 2073 (2007).

[32] B.K. Sharma, P. Arumugam, S.K. Patra, P.D. Stevenson, R.K. Gupta and W. Greiner, J. Phys. G: Nucl. Part. Phys. **32**, L1 (2006).

[33] R.K. Gupta, S.K. Patra, P.D. Stevenson and W. Greiner, Int. J. Mod. Phys. E **16**, 1721 (2007).

[34] E. Chabanat, P. Bonche, P. Hansel, J. Meyer and R. Schaeffer, Nucl. Phys. A **627**, 710 (1997).

[35] J.R. Stone and P.-G. Reinhard, Prog. Part. Nucl. Phys. **58**, 587 (2007).

[36] J.R. Stone, J.C. Miller, R. Koncewicz, P.D. Stevenson and M.R. Strayer, Phys. Rev. C **68**, 034324 (2003).

[37] P.-G. Reinhard and H. Flocard, Nucl. Phys. A **584**, 467 (1995).

[38] E. Chabanat, P. Bonche, P. Haensel, J. Meyer and R. Schaeffer, Nucl. Phys. **A635**, 231 (1998).

[39] B.A. Brown, Phys. Rev. **C58**, 220 (1998).

[40] S.J. Krieger, P. Bonche, H. Flocard, P. Quentin and M.S. Weiss, Nucl. Phys. A **517**, 275 (1990).

[41] B.D. Serot and J.D. Walecka, Adv. Nucl. Phys. **16**, 1 (1986).

[42] Y.K. Gambhir, P. Ring and A. Thimet, Ann. Phys. (N.Y.) **198**, 132 (1990).

[43] S. K. Patra and C. R. Prahara, Phys. Rev. **C44**, 2552 (1991).

[44] C. E. Price and G. E. Walker, Phys. Rev. C **36**, 354 (1987).

[45] Y. Sugahara and H. Toki, Nucl. Phys. A **579**, 557 (1994).

[46] P.K. Panda, S.K. Patra, J. Reinhardt, J.A. Maruhn, H. Stöcker and W. Greiner, Int. J. Mod. Phys. E **6**, 307 (1997).

[47] S. Gmuca, Nucl. Phys. A **547**, 447 (1992).

[48] G.A. Lalazissis, J. König and P. Ring, Phys. Rev. **C55**, 540 (1997).

[49] T.L. Khoo *et al.* Phys. Rev. Lett. **76**, 1583 (1996).

[50] E. Uegaki and Y. Abe, Phys. Lett. B **340**, 143 (1994).

[51] H. Feldmeier and J. Schnack, Rev. Mod. Phys. 72, 655 (2000).